Proceedings of The Korean Nuclear Society Spring Meeting
Ulsan, Korea, May 1995

Thermal Aging Embrittlement in LWR Primary Pressure Boundary Components

Sunki Kim, Yongsoo Kim, and Wonmok Jae
Hanyang University

Abstract

Two techniques for the verification of the phase separation in ferrite phase of primary pressure bounary component materials, the primary cause of thermal aging embrittlement, are presented. Data base of room-temperature Charpy V-notch impact energy during reactor service was estimated as a measure of the degree of embrittlement. The serviceable period of CF-3 and CF-8 alloys as the primary pressure boundary components may be acceptably extended for 60 years of lifetime. However, the integrity of CF-8M alloys can be degraded seriously after several years of service in the nuclear reactor.

1. Introduction

Cast duplex stainless steels, composed of austenite and ferrite phases, are used extensively for primary pressure boundary components such as primary coolant pipe, valves, and pump casings and weld filler metal in LWRs. The ferrite phase in the duplex structure of austenitic and ferritic stainless steel increases the tensile strength and improves weldability, resistance to stress corrosion cracking, and soundness of castings of these steels. The superior properties of the cast stainless steels result primarily from the presence of the ferrite phase in the duplex structure. On the other hand, it has long been known that ferritic stainless steels are susceptible to severe embrittlement when exposed to temperatures in the range of 300 ~ 500°C owing to the precipitaion of the α' phase[1-3].

It was reported that primary pressure boundary components such as hot leg elbow, main valve, and recirculation pump cover decommissioned from Ringhals Unit 2, Shippingport PWR, and KRB BWR had suffered severe degradation of impact property[4,5].

The possibility of the significant embrittlement of cast stainless steel has been confirmed by recent studies on cast materials that were aged at temperatures of 300 ~ 450°C for times up to 70,000h. Because realistic aging of the components at the end of lifetime at 280 ~ 330°C cannot be produced in the laboratory, it is customary to simulate it by accelerated aging at 400°C. Therefore, it is important to validate that the mechanisms of the aging embrittlement are identical for the accelerated aging and reactor operating conditions. The primary and secondary aging processes were found to be identical to those of the laboratory-aged specimens, and the characteristics of the kinetics were similar. Until recently, the embrittlement of aged cast stainless steels was attributed primarily to Cr-rich α' precipitation by spinodal decomposition.

In the previous investigations, transmission electron microscopy (TEM), small angle neutron scattering (SANS), and atom probe field ion microscopy (APFIM) results show that several metallurgical processes can be causes of aging embrittlement of the ferrite phase of duplex stainless steel. They are precipitation of G phase, γ_2 phase, α' phase by spinodal decomposition, and $M_{23}C_6$. Analysis of microhardness and toughness recovery and microstructural evolution of aged specimens following an annealing treatment at 550°C showed that the primary mechanism for the thermal aging embrittlement is the spinodal decomposition of the ferrite.

In the present paper, phase separation into α phase and α' phase is identified Mössbauer spectra analysis and saturation magnetization measurement using vibrating specimen magnetometer (VSM). The degree of embrittlement during reactor service time is estimated and compared for ASME SA 351 grade CF-3, CF-8, and CF-8M.

2. Identification of Phase Separation

Analysis of Mössbauer spectra and saturation magnetization measurement using vibrating specimen magnetometer (VSM) were carried out to identify phase separation into Fe-rich and Cr-rich regions. The Mössbauer spectra result from the absorption of γ-rays by Fe iron nuclei. When these nuclei are in ferromagnetic environments, such as in α-iron below the Curie point, a six line absorption spectrum is observed. The separation between the lines or peaks is proportional to the hyperfine field of the iron nucleus. If the ^{57}Fe nucleus is in a paramagnetic environment, then a single paramagnetic peak, located near zero velocity, will be observed. If both ferromagnetic and paramagnetic phases are present in an alloy then the observed spectrum will be the superposition of the 6 peak ferromagnetic spectrum and the single peak paramagnetic spectrum.

The hyperfine field, the characteristic of ferromagnetic ^{57}Fe, can be characterized by the spacing between outmost 6 ferromagnetic peaks. The Mössbauer spectra for specimens aged up to 5,064h at 370°C is shown in Figure 1. The peak positions were determined by Lorentzian curve fitting. Formation of appreciable paramagnetic peak was not observed in Mössbauer spectra. 5,064h aging at 370°C seems to be not enough to form a paramagnetic peak. Since no paramagnetic phase is being formed during 5,064 hours at 370°C, no paramagnetic peak will thus be formed in conjunction with the increase of hyperfine field. Eventually, however, at the end of the spinodal decomposition the equilibrium α' phase will form from Cr rich regions.

Figure 2 shows a increase of the hyperfine field with aging time. The hyperfine fields of Fe nuclei are altered by altering the environment of the nuclei. The addition of Cr atoms reduces the hyperfine field. Mössbauer effect measurements can therefore be used to determine the environment of Fe nuclei in the alloy. Figure 3 shows the hyperfine field vs. chromium content as determined by Johnson *et al.*[6]. An almost identical curve would be drawn through the data of Yamamoto[7], De Nys and Gielen[8] and Roy and Solly[9]. The hyperfine field for unaged specimen used in the present experiment is in agreement with Johnson *et al.* It is observed that the hyperfine field decreases with increasing Cr content.

From Figure 3, it can be seen that the hyperfine field after aging time of 5,064 hours is about 280kOe. The value of 280kOe corresponds to about 20 at.% Cr (18 wt.% Cr), which is not equilibrium Cr content in the α phase. There seems to be some tendency for the hyperfine field to approach the same value of about 290kOe that corresponds to about 15 at. % Cr (13wt.% Cr). This observation is indicative of proceeding phase separation into Fe-rich regions and Cr-rich regions, therefore, equilibrium α' phase was not formed yet. Since Cr is leaving the α phase, the number of Cr atoms neighboring Fe atoms will decrease and concomitantly the numbers of Fe neighbors will increase. This causes an increase of the hyperfine field of Fe nuclei in the ferromagnetic α phase. The contribution of the ^{57}Fe absorption from Cr-rich regions will be less than that from the Fe-rich regions because there is less ^{57}Fe present. This causes an apparent increase of the hyperfine field during spinodal decompositon.

Variations in specific saturation magnetization with aging time at 370 and 400°C is shown in Figure 4 and 5, respectively. It can be seen that specific saturation magnetization increases with increasing Fe content. This is due to ferromagnetic property of Fe. Increase in specific

saturation magnetization is also observed for all specimens with increasing aging time. This fact is indicative of Fe-content increase in α phase with aging time, that is, phase separation into Fe-rich regions and Cr-rich regions is proceeding with increasing aging time. This can be explained by molecular theory and exchange energy of ferromagnetic elements.

Much higher increase in specific saturation magnetization is especially observed for HY3 and HY4 containing Ni compared with other specimens. The rate of spinodal decomposition in ternary alloy is controlled by the interdiffusion coefficient. The influence of Ni on Fe-Cr interdiffusion seems to play an important role.

3. Estimation of Thermal Aging Embrittlement during Reactor Service

A procedure and correlations for assessing thermal embrittlement and predicting Charpy impact energy of cast stainless steel components during reactor service have been developed by Chopra and Shack[10] of Argonne National Laboratory (ANL). Mechanical properties of a specific cast stainless steel are estimated from the extent and kinetics of thermal embrittlement. Embrittlement of cast stainless steel is characterized in terms of room-temperature Charpy impact energy . The extent or the degree of thermal embrittlement at "saturation", i.e., the minimum impact energy that can be achieved for the material after long-term aging, is determined from chemical composition of the steel.

Charpy impact energy as a function of time and temperature of reactor service is estmated from the kinetics of thermal embrittlement, which is also determined from the chemical composition. The initial impact energy of the unaged steel is required for these estimations.

$$P = \log_{10}\{t / \exp[(Q/R)(1/T - 1/673)\}, \quad (1)$$

where t is the reactor service time(hour), Q is the activation energy, R is the gas constant, and T is the service temperature(K). Aging parameter, P, is defined such that it is equivalent to the logarithm of the number of hours of aging at 400°C. The RT impact energy as a function of time and temperature of aging of a specific cast stainless steel is determined from its estimated RT saturation impact enrgy Cv_{sat} and the kinetics of embrittlement. The decrease in RT Charpy impact energy Cv with aging time is expressed as:

$$\log_{10} Cv = \log_{10} Cv_{sat} + ß\{1 - \tanh [(p - \theta)/\alpha]\}. \quad (2)$$

The constants α and ß can be determined from Cv_{int} and Cv_{sat} and the values of θ varies with service temperature. The activation energy, Q, is given in terms of both chemical composition and the constant θ. Using above correlations, variations in RT Charpy impact energy for grade CF-3, CF-8, and CF-8M during reactor service time were plotted in Figure 6,7, and 8. CF-8M shows the widest spread in predicted Charpy impact energy values and it is most affected by thermal aging. CF-3 was found to be least affected by thermal aging. CF-8 falls between CF-3 and CF-8M. The horizontal dotted line in Figure 8 corresponds to the lower bound RT Charpy impact energy of 35.3 J/cm^2 recommended by Framatome[11]. For a 40-year period, CF-3 and CF-8 fall above the 35.3 J/cm^2 lower bound Charpy impact energy, but some of the CF-8M compositions are predicted to fall below the recommended lower bound. Based on this model and Framatome recommendation, CF-3 and CF-8 alloys are predicted to provide acceptable service for extended lifetime of 60 years. However, for some of the CF-8M compositions potential problems are predicted after several years of service.

4. Conclusions and Recommendations

The formation of the α' phase is primary cause of the embrittlement in primary pressure boundary components at LWR operating temperatures. Mössbauer spectrometer and vibrating specimen magnetometer (VSM) have verified the phase separation into Fe-rich regions and Cr-rich regions.

The CF-3 and CF-8 alloys are predicted to provide safe performance during extended lifetime of 60 years as well as designed lifetime of 40 years, but for some of the CF-8M compositions potential problems are predicted after several years of service. Tight in-service inspection (ISI) of CF-8M alloys may be required to secure the integrity of primary pressure boundary components since most of primary coolant piping materials in domestic nuclear power plants is CF-8M.

References

[1] H.M. Jung, *ASME PVP* **171** (1989) 111
[2] C. Jasson, *Proc. Fontevraud II Int'l. Symp. Fontevraud, France* (Sept.1990)
[3] O. K. Chopra and H. M. Jung, *Nucl. Eng. and Desg.*, **89** (1985) 305
[4] H. M. Jung and T. R. Leak, *International Workshop on Intermediate Temp. Embrittlement Process in Duplex Stainless Steel, Oxford, England* (Aug. 1989)
[5] O. K. Chopra and H. M. Jung, *Proc. 16th Water Reactor Safety Information Meeting, Gaithersburg* (Oct.1988)
[6] C. E. Johnson, M. S. Ridout, and T. E. Cranshaw, *Proc. Phys. Soc.*, **81** (1963) 1079
[7] H. Yamamoto, *Japan J. Appl. Phys.*, **3** (1964) 745
[8] T. De Nys and P. M. Gielen, *Metall. Trans.*, **2** (1971) 1423
[9] R. B. Roy and B. Solly, *Scand. J. Metallurgy*, **2** (1973) 243
[10] O. K. Chopra and W. J. Shack, *NUREG/CR-6177* (1994)
[11] C. E. Jaske and V. N. Shah, *Life Assessment Procedure For LWR Cast Stainless Steel Components*

Heats	Cr	Ni	Si	Fe
HY1	25	-	-	Bal.
HY2	30	-	-	Bal.
HY3	30	5	-	Bal.
HY4	30	5	2	Bal.

Table 1. Chemical compositions of specimens

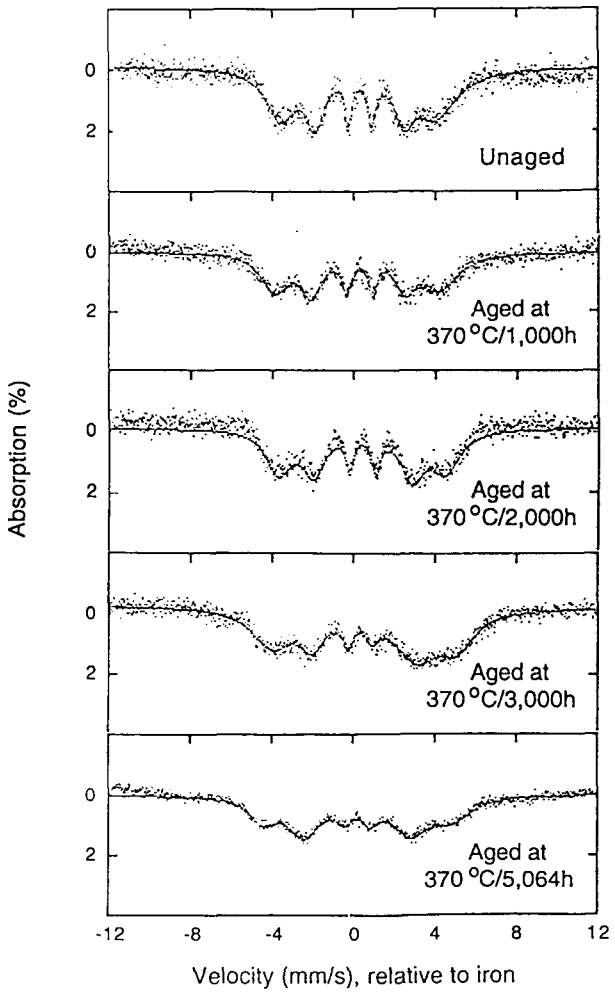

Figure 1 Mössbauer spectra for thermally aged Fe-30Cr steels at 370°C

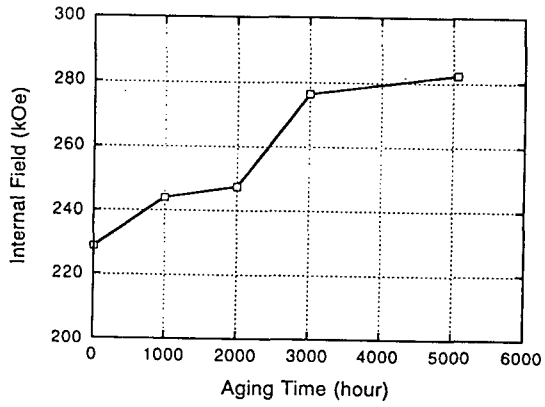

Figure 2. Hyperfine field for thermally aged Fe-30Cr steels at 370°C

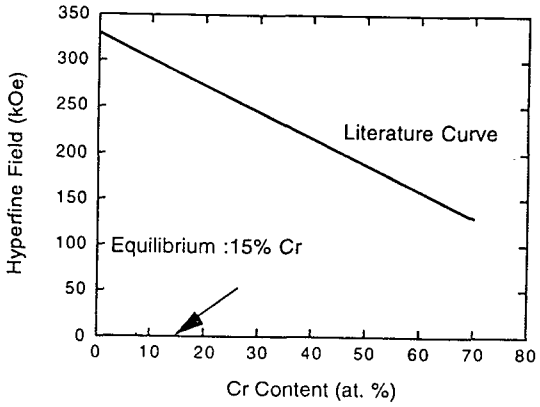

Figure 3. Hyperfine field vs. Cr content for binary Fe-Cr alloys

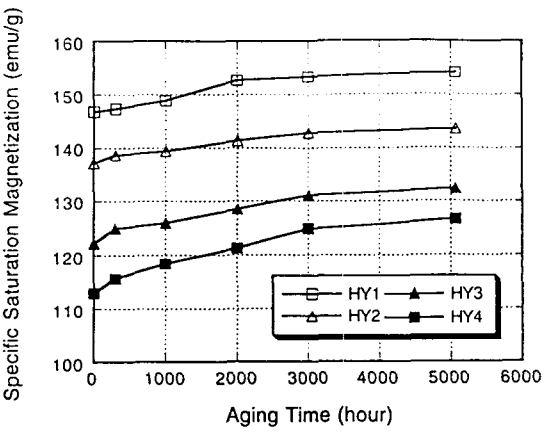

Figure 4. Specific saturation magnetization as a function of aging time at 370°C

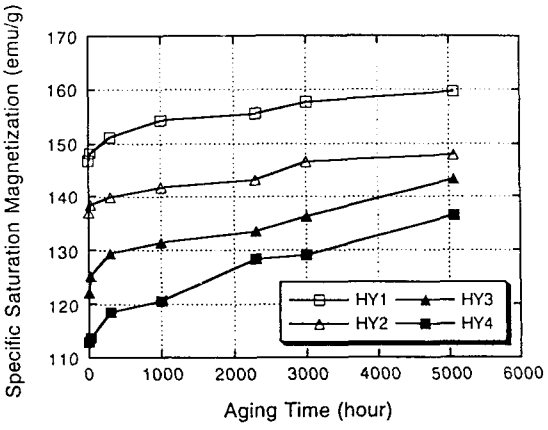

Figure 5. Specific saturation magnetization as a function of aging time at 370°C

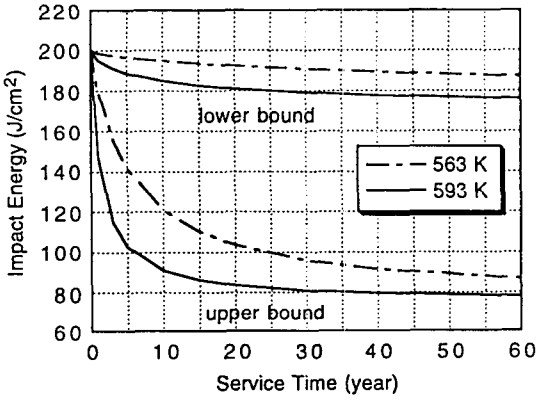

Figure 6. Predicted RT Charpy V-notch impact energy for CF-3 grade cast stainless steel as a function of service time

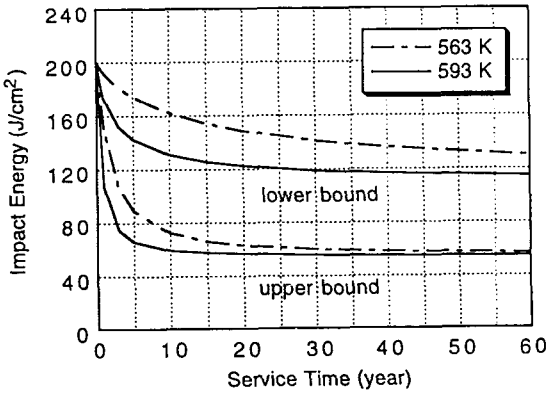

Figure 7. Predicted RT Charpy V-notch impact energy for CF-8 grade cast stainless steel as a function of service time

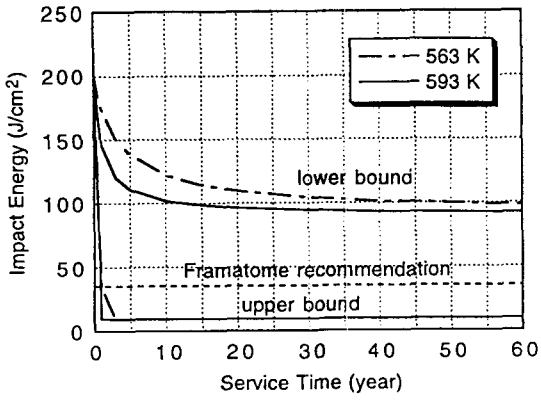

Figure 8. Predicted RT Charpy V-notch impact energy for CF-8M grade cast stainless steel as a function of service time